# Numerical study of the dynamical aspects of pattern selection in the stochastic Swift-Hohenberg equation in one dimension

Jorge Viñals
*Supercomputer Computations Research Institute, B-186, Florida State University, Tallahassee, Florida 32306-4052 and Departament de Física, Universitat de les Illes Balears, 07071 Palma de Mallorca, Spain*

Emilio Hernández-García,* Maxi San Miguel, and Raúl Toral
*Departament de Física, Universitat de les Illes Balears, 07071 Palma de Mallorca, Spain*
(Received 29 January 1991)

We solve numerically both the deterministic and stochastic Swift-Hohenberg equation [J. Swift and P.C. Hohenberg, Phys. Rev. A **15**, 319 (1977)] in one spatial dimension. In the deterministic case we address the question of pattern selection by studying the temporal evolution away from a uniform, unstable solution. The asymptotic stationary solutions found are periodic in space with a range of wave numbers that is narrow, and consistent with earlier theoretical predictions on the range of allowable periodicities in a finite system. In the stochastic case, the power spectrum of the stationary solutions is very broad and typical configurations do not have a well-defined periodicity. A correlation length is defined that measures the extent over which a stationary solution is periodic. We find that the correlation length is finite, smaller than the size of the system studied and decreases with the amplitude of the stochastic contribution. We confirm these findings by performing a Monte Carlo heat-bath simulation that directly samples the stationary probability distribution function associated with the Lyapunov functional from which the Swift-Hohenberg equation is derived.

## I. INTRODUCTION

We present, in this paper, a numerical study of both the transient and stationary solutions of the stochastic Swift-Hohenberg equation in one spatial dimension [1]. This equation describes the temporal evolution of a dynamical variable $y(x,t)$, the function of a space variable $x$, and time $t$,

$$\frac{\partial y(x,t)}{\partial t} = \left[\gamma^2 - \left(1+\frac{\partial^2}{\partial x^2}\right)^2\right] y(x,t) - y(x,t)^3 + \xi(x,t) , \tag{1}$$

where $0 \le x \le L$. The variable $\xi(x,t)$ is a Gaussian stochastic process defined by

$$\langle \xi \rangle = 0, \quad \langle \xi(x,t)\xi(x',t') \rangle = 2\epsilon' \delta(x-x')\delta(t-t') . \tag{2}$$

The constant $\gamma$ plays the role of a control parameter such that for $\gamma^2 < 0$ the solution $y(x) = 0$ is linearly stable, and unstable otherwise. At $\gamma = 0$ the solution $y(x) = 0$ becomes marginally unstable. For $\gamma^2 > 0$, and in the limit of vanishing $\epsilon'$, stationary solutions $y_q(x)$ exist that are periodic in $x$ with wave number $q$. We will be exclusively concerned in this paper with the case $\gamma^2 > 0$. The Swift-Hohenberg equation was originally introduced to model the onset of a convective instability in simple fluids (Rayleigh-Bénard instability). The stationary solution $y(x) = 0$ corresponds to the conducting state below the convective instability. The onset occurs at $\gamma^2 = 0$, leading to a stationary convective state consisting of rolls of wavelength $\lambda = 2\pi/q$. We restrict ourselves in the present work to the one-dimensional equation that can only model the appearance of straight and parallel convective rolls. More complex patterns that appear under a variety of conditions may be modeled by the same equation in two spatial dimensions. The extension of our results to higher dimensions will be discussed separately.

Most of the theoretical studies of the Swift-Hohenberg equation have focused on the deterministic equation ($\epsilon' = 0$). If thermal fluctuations are the only source of random fluctuations in the fluid, the value of $\epsilon'$ is inversely proportional to the characteristic wavelength of the convective rolls (in thin convective cells) and is thought to be very small for simple fluids ($\sim 10^{-9}$) [2]. Hence its contribution to Eq. (1) has been normally neglected. Important work in which nonzero $\epsilon'$ has been considered includes the original derivation of the equation to model the effect of hydrodynamic fluctuations on the onset of the instability [1], a study of the dynamical amplification of the fluctuations after the instability [2], and the analysis of the influence of the fluctuations on pattern selection [3]. On the other hand, recent experimental studies of an electrohydrodynamic convective instability in nematic liquid crystals reports patterns of rolls of a few micrometers wide [4]. As a consequence, the value of $\epsilon'$ in that system could be several orders of magnitude larger than in simple fluids and the effects of random fluctuations more readily accessible to experimental observation.

Our study of the stochastic Swift-Hohenberg equation is motivated, in part, by the issue of pattern selection in the presence of random fluctuations. In the absence of fluctuations and in a finite geometry, it is known that the

 

nature of the stationary solutions and their periodicity strongly depend on the choice of boundary conditions [5]. We have, instead, studied the selection process in an infinite geometry and allowed for random fluctuations in Eq. (1). In particular, we have analyzed the competition among the different stable stationary solutions allowed in a system with periodic boundary conditions.

We study in this paper the onset of a convective instability and the evolution of the ensuing pattern of convective rolls, both for $\epsilon' = 0$ and $\epsilon' > 0$, in a large aspect ratio system (i.e., a system comprising a large number of convective rolls). In terms of the Swift-Hohenberg equation, we take the unstable solution $y(x) = 0$ as the initial condition and numerically solve Eq. (1) to obtain $y(x,t)$. For $\epsilon' = 0$ an initial random perturbation is added at $t = 0$. At times long enough, $y(x,t)$ is seen to converge to a periodic stationary solution $y_q(x)$ [6] that depends on the initial random perturbation [7].

The wave number $q$ falls within a well-defined range that is centered around the wave number of the mode of fastest growth during the linear regime after the instability. This range is approximately equal to the range calculated in a one-dimensional finite system [5, 8], even though, as we will make explicit below, our choice of boundary conditions is different. For $\epsilon' \neq 0$, the final stationary solution no longer depends on the initial condition. After the initial regime, well described by the linear approximation, the Fourier transform of $y(x,t)$,$\tilde{y}(q,t)$ exhibits a number of peaks at different values of $q$ that alternatively dominate at different times. At sufficiently long times, the solutions appear to be stationary in a statistical sense. We show that in that time regime characteristic configurations do not have long-ranged periodicity. The absence of periodicity manifests itself in several different ways. First, we have calculated a local power spectrum by defining spatial windows at different locations $x_0$ and of varying width. The local spectrum is dominated by different wave numbers for different $x_0$; hence the characteristic stationary solutions comprise regions of different periodicities. Second, we have calculated a correlation length that describes the average size of the region over which the solution can be well described by a single periodic function. We have found this length to be much smaller than $L$. We further characterize the transient states by giving the time dependence of the average correlation length for different values of $\epsilon'$.

The outline of the paper is the following. In Sec. II the Swift-Hohenberg model is briefly reviewed. We also discuss the deterministic stationary solutions, their stability limits, and the dynamical evolution away from an unstable initial condition. Section III presents our results for $\epsilon' \neq 0$, both the transient evolution away from the unstable state and the asymptotic stationary solution. This stationary solution is also compared in Sec. III with ensemble averages obtained by Monte Carlo methods.

## II. MODEL AND SOLUTIONS OF THE DETERMINISTIC EQUATION

We first briefly review some known results about the deterministic Swift-Hohenberg equation, i.e., $\epsilon' = 0$. For small $\gamma$ (close but above the onset of instability), Eq. (1) has periodic stationary solutions characterized by a wave number $q$, and given by [9]

$$y_q(x) = \sum_{i=0}^{\infty} A_i(q) \sin[(2i+1)qx] \ . \tag{3}$$

By direct substitution of Eq. (3) into Eq. (1) (with the left-hand side equal to zero) and for wave numbers $q \approx 1$, one can show that $A_i(q)$ is of order $\gamma^{2i+1}$. The first two coefficients are given by

$$A_0(q) = \sqrt{\tfrac{4}{3} w(q)} \tag{4}$$

and

$$A_1(q) = -\frac{A_0(q)^3}{4w(3q)} \ , \tag{5}$$

where we have introduced

$$\omega(q) = \gamma^2 - (q^2 - 1)^2 \ . \tag{6}$$

These solutions only exist in the range of wave numbers determined by $\omega(q) \geq 0$, i.e., for $q \in [q_{-L}, q_L]$, $q_{\pm L} = \sqrt{1 \pm \gamma}$. For large $\gamma$ the stationary solutions have to be found numerically. We have used the stationary solutions, both for small and large $\gamma$, to test the accuracy of the numerical procedure which we will describe below [10].

The stability of the various stationary solutions against certain perturbations is also well known. The stationary solution $y(x) = 0$ is linearly unstable against perturbations of wave number $q$ such that $\omega(q) > 0$ [$\omega(q) = 0$ is the neutral stability curve]. The mode of fastest growth, $q_0$, is given by $\partial\omega/\partial q|_{q=q_0} = 0$ and corresponds, in the dimensionless form of Eq. (1), to $q_0 = 1$. On the other hand, only a subset of the periodic solutions with $q_{-E} \leq q \leq q_E$ is stable ($q_{-L} < q_{-E} < q_E < q_L$). Solutions with $q$ outside this range are unstable against a long-wavelength instability known as the Eckhaus instability [11]. The value of $q_E$ can be determined approximately for small $\gamma$, or numerically for any $\gamma$ [9, 12]. In the region of small $\gamma$ ($\gamma \leq 0.5$), we found both results to agree very well. It is found that $q_{\pm E} \simeq (q_{\pm L} - 1)/\sqrt{3} + 1$.

The issue of pattern selection concerns the determination of the stable stationary solution that corresponds to a given initial condition. It is commonly argued in the case of the Swift-Hohenberg equation that selection follows from a variational principle. In fact, Eq. (1) can be rewritten as

$$\frac{\partial y(x,t)}{\partial t} = -\frac{\delta \mathcal{L}(\{y\})}{\delta y(x,t)} + \xi(x,t) \ , \tag{7}$$

where the Lyapunov functional $\mathcal{L}(\{y\})$ is given by

$$\mathcal{L}(\{y\}) = \int_0^L dx \left[ -\frac{\gamma^2 - 1}{2} y^2 + \frac{1}{4} y^4 - \left(\frac{\partial y}{\partial x}\right)^2 + \frac{1}{2}\left(\frac{\partial^2 y}{\partial x^2}\right)^2 \right] . \tag{8}$$

$\delta/\delta y(x,t)$ stands for the functional derivative with re-

spect to $y(x,t)$ and $L$ is large ($q_0 L \gg 1$). The boundary conditions on $y(x,t)$ are

$$y(0,t) = y(L,t) = 0, \quad \frac{\partial y}{\partial x}(0,t) = \frac{\partial y}{\partial x}(L,t) = 0 \ . \tag{9}$$

Under these conditions, the solution that minimizes $\mathcal{L}$ is the most probable solution if $\epsilon' \neq 0$, and is also argued to be the selected solution for any initial condition when $\epsilon' = 0$ [6]. This solution, except for boundary layer contributions near $x = 0$ and $L$, is periodic with a wave number $q_{\min} = q_0 - \gamma^4/1024 q_0^7 \simeq 0.999\,94$ [9], again for $\gamma = 0.5$. It has also been shown that this choice of boundary conditions further restricts the range of allowed solutions to wave numbers $q_- \leq q \leq q_+$ ($q_{-E} < q_- < q_+ < q_E$), with $q_\pm = q_0 \pm \gamma^2/16 q_0^3$ [8,5]. According to this view, the periodicity of the solution can be continuously adjusted by creating or removing rolls near the boundaries (where $y$ is small) until the periodicity that minimizes $\mathcal{L}$ is reached.

Other selection mechanisms have been proposed that are dynamical in nature. When the initial condition is such that a localized region of a stable solution [$y_q(x) \neq 0$] is surrounded by a large region of the unstable solution [$y(x) = 0$], selection takes place dynamically at the moving front separating both regions, according to the marginal stability hypothesis [13, 14]. If the initial condition is not localized, a singular perturbation expansion [15] yields a selected wave number equal to $q_0$ (for a localized initial condition, the results from this expansion are consistent with the marginal stability hypothesis at the front, but not well inside the region occupied by the stable periodic solution). The effect of random fluctuations during the transient evolution and its effect on the selection process has not been considered, even though they may be essential if the variational principle is to dictate the selected stationary solution. We note, however, that our numerical accuracy is not enough to distinguish between $q_{\min}$ and $q_0$.

We next describe the details of our numerical study. We consider periodic boundary conditions on $y(x,t)$

$$y(0,t) = y(L,t) \tag{10}$$

for all times because we are primarily interested in the case $\epsilon' > 0$. As we shall discuss in more detail in Sec. III, the stationary solutions in that case can be locally approximated by periodic functions, but this is true over ranges of $x$ much smaller than $L$ for the values of $\epsilon'$ that we have considered. Consequently, we do not expect that the choice of boundary conditions will affect the results and conclusions presented in that section. For completeness, we analyze in the present section the transient and stationary solutions of the deterministic equation with periodic boundary conditions.

Space and time are discretized and $y(x,t)$ represented by a finite number of variables, $\{y_i(t)\}$ ($i = 1, \ldots, N$) equally spaced in $x$, with $\Delta x = L/N$. In some cases, we will refer to the set $\{y_i(t)\}$ at a given time as a configuration. All our calculations consider $N$=8192, although occasionally we have studied the cases $N$=1024 or 512. After solving numerically the partial differential equation that gives the stationary solutions of the Swift-Hohenberg equation, we have found that a value for the spatial discretization $\Delta x \leq 2\pi/32$ is needed in order to obtain stationary solutions that are, to a good approximation, independent of $\Delta x$. We have chosen $\Delta x = 2\pi/32$ in all our calculations. Periodic boundary conditions lead to a discretization of wave numbers $\Delta q = 2\pi/L = 2\pi/N\Delta x = 0.0039$ for $N$=8192 and $\Delta q = 0.031$ for $N$=1024. With this choice of parameters, the stationary periodic solutions corresponding to $N$=8192 are comprised of the order of 256 periods or 512 nodes [a node is a point at which the solution $y(x,t)$ vanishes]. We use an explicit integration scheme in time. Given the nature of the equation, the discretization in time $\Delta t$ has to satisfy $\Delta t \sim O(\Delta x^4)$ for stability considerations. We have chosen $\Delta t = 10^{-4}$ in all our calculations. Spatial derivatives are approximated by finite differences up to $O(\Delta x)^4$. The finite-difference approximation to Eq. (1) is

$$y_i(t+\Delta t) - y_i(t) = \Delta t \left[ (\gamma^2 - 1) y_i(t) - \frac{2}{(\Delta x)^2} \left( \hat{\delta}^2 y_i - \frac{1}{12} \hat{\delta}^4 y_i \right) \right] - \Delta t \left[ \frac{1}{(\Delta x)^4} \hat{\delta}^4 y_i + y_i^3 \right] + f_i(t) \ , \tag{11}$$

where $\hat{\delta}$ is the central difference operator $\hat{\delta} y_i = y_{i+1/2} - y_{i-1/2}$. Although in this section we are only concerned with the case $\epsilon' = 0$, we have also included Eq. (11) for later reference the random contribution $f_i(t)$ given by

$$f_i = \sqrt{\frac{2\epsilon' \Delta t}{\Delta x}}\, \eta_i \equiv \sqrt{\epsilon \Delta t}\, \eta_i \ , \tag{12}$$

where the variables $\eta_i$ are Gaussian random variables, such that $\langle \eta_i \rangle = 0$ and $\langle \eta_i \eta_j \rangle = \delta_{ij}$ ($\delta_{ij}$ is the Kronecker $\delta$).

In order to study the evolution away from the unstable solution $y(x) = 0$, we choose as the initial condition a linear superposition, with random complex coefficients, of all the modes $\hat{y}(q,t)$ such that $\omega(q) > 0$. The random coefficients are taken to be small so that, typically, the maximum amplitude of the initial condition is $|y(x,0)| \sim 10^{-2}$. We have studied an ensemble of such initial conditions and in some cases averaged the results obtained over the ensemble. In this latter case, we normally average our results over 15–20 independent initial conditions.

We characterize the transient dynamics by the power spectrum of $y_i(t)$ defined as

$$P(q,t) = \frac{1}{N} \left| \sum_{i=1}^{N} y_i(t) e^{-iqx_i} \right|^2 \ , \tag{13}$$

where $x_i = (i-1)\Delta x$. For a given initial condition the power spectrum is seen to evolve from its initial value at $t = 0$ to a $\delta$ function centered around a particular value of $q$ at late times. The value of $q$ falls within a very narrow range and depends on the initial condition. In this evolution one can distinguish an initial linear regime from an intermediate nonlinear regime. In this latter regime, the amplitude of $y(x,t)$ saturates and the width of $P(q,t)$ decreases with increasing $t$, thus indicating that the solution is evolving towards a configuration characterized by a unique wavelength. We have also investigated the evolution of the power spectrum averaged over initial conditions in order to gain insight on the distribution of the wave vectors that are statistically dominant at late times. Figure 1 shows the evolution of the power spectrum averaged over 15 independent initial conditions. As expected, the fastest growing mode in the linear regime ($q_0$=1) dominates at early or intermediate times. At late times the power spectrum narrows but remains centered around the same value of $q$. We show in Fig. 2 the position of $q_{\max}$, the wave number for which the average of $P(q,t)$ is maximum, as a function of time. We find that at the latest time studied, $q_{\max} = 1.006 \pm 0.005$ ($N$=1024, $t$=500) or $q_{\max} = 1.005 \pm 0.005$ ($N$=8192, $t$=100). The error estimate is obtained from the standard deviation $\sigma$ of the values of $q_{\max}$ obtained for the $n$ different runs: $\sigma/\sqrt{n}$. This figure also shows the number of nodes of $y_i(t)$ as a function of time, averaged over the same number of independent runs. After an initial transient, the average number of nodes remains approximately constant in time. We find that the average number of nodes is 64.375 ($N$=1024, $t$=500), which for a periodic function would correspond to a wave number $q$=1.006, and 513.2 ($N$=8192, $t$=100) which corresponds to $q$=1.002. These results are consistent within our numerical accuracy with a selected wave number $q = q_0$.

In summary, our results indicate that the long-time solutions of Eq. (1), with our choice of boundary and initial conditions, are periodic with wave number $q$. We find a range of values of $q$ for a distribution of initial condi-

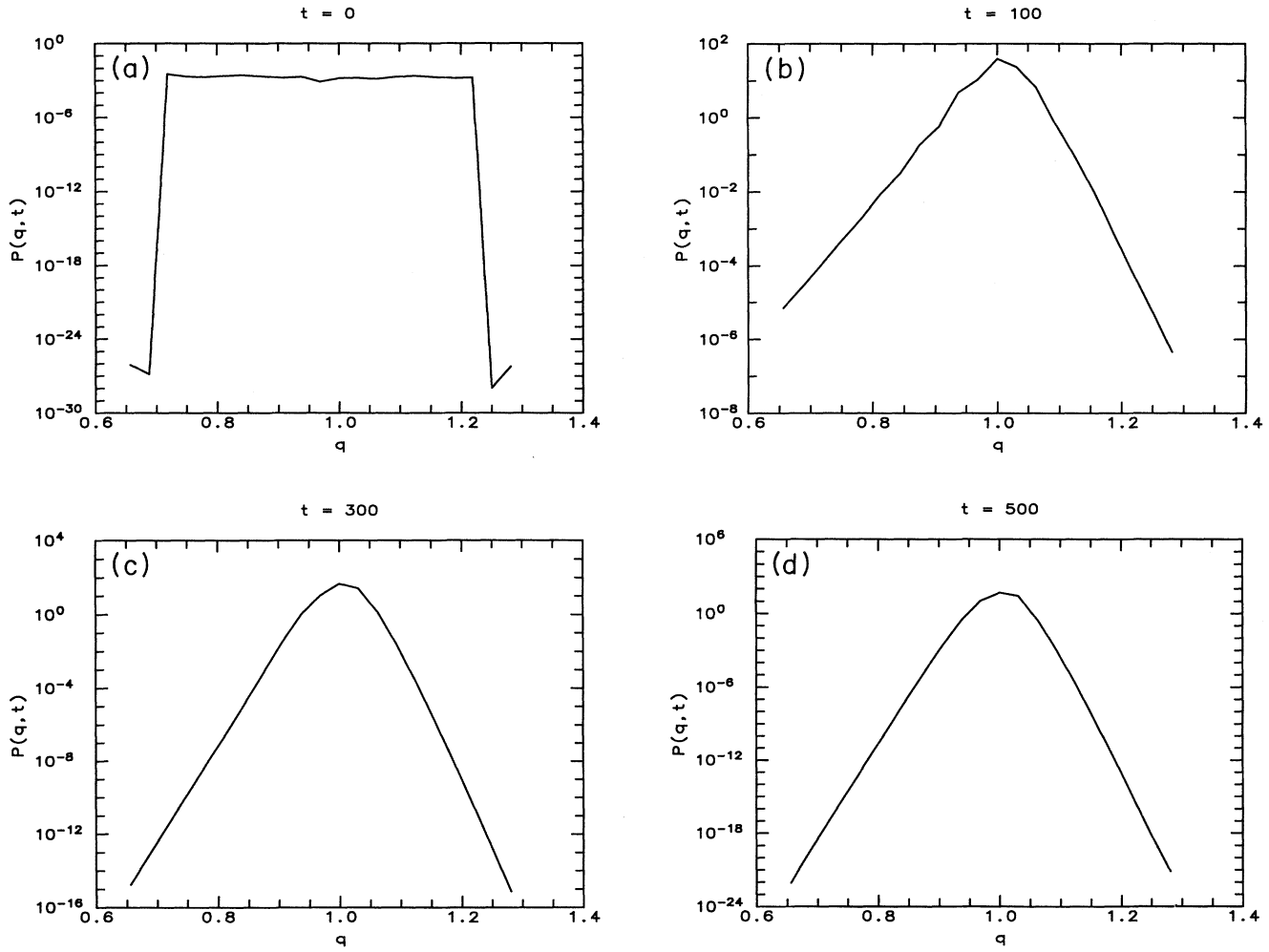


FIG. 1. Power spectrum $P(q,t)$ averaged over 15 independent runs, for $\epsilon$=0 and $N$=1024 at different times after the instability. (a) $t$=0, (b) $t$=100, (c) $t$=300, and (d) $t$=500.

tions, as indicated above. This range is very narrow and, within our numerical accuracy, is centered around $q_0$ and substantially smaller than $[q_{-E}, q_E]$, presumably in part because the exponential amplification during the linear regime acts to suppress modes with periodicities different than $q_0$. We further note that for $\gamma=0.5$, $q_+ - q_- \simeq 0.03$, a value that is close to the standard deviations that we have obtained ($\sigma=0.02$). We note that the analysis described in Refs. [8] and [5] considers the boundary conditions given in Eq. (9) and therefore it does not strictly apply to our case. However, at early or intermediate times after the instability, we observe regions of rather

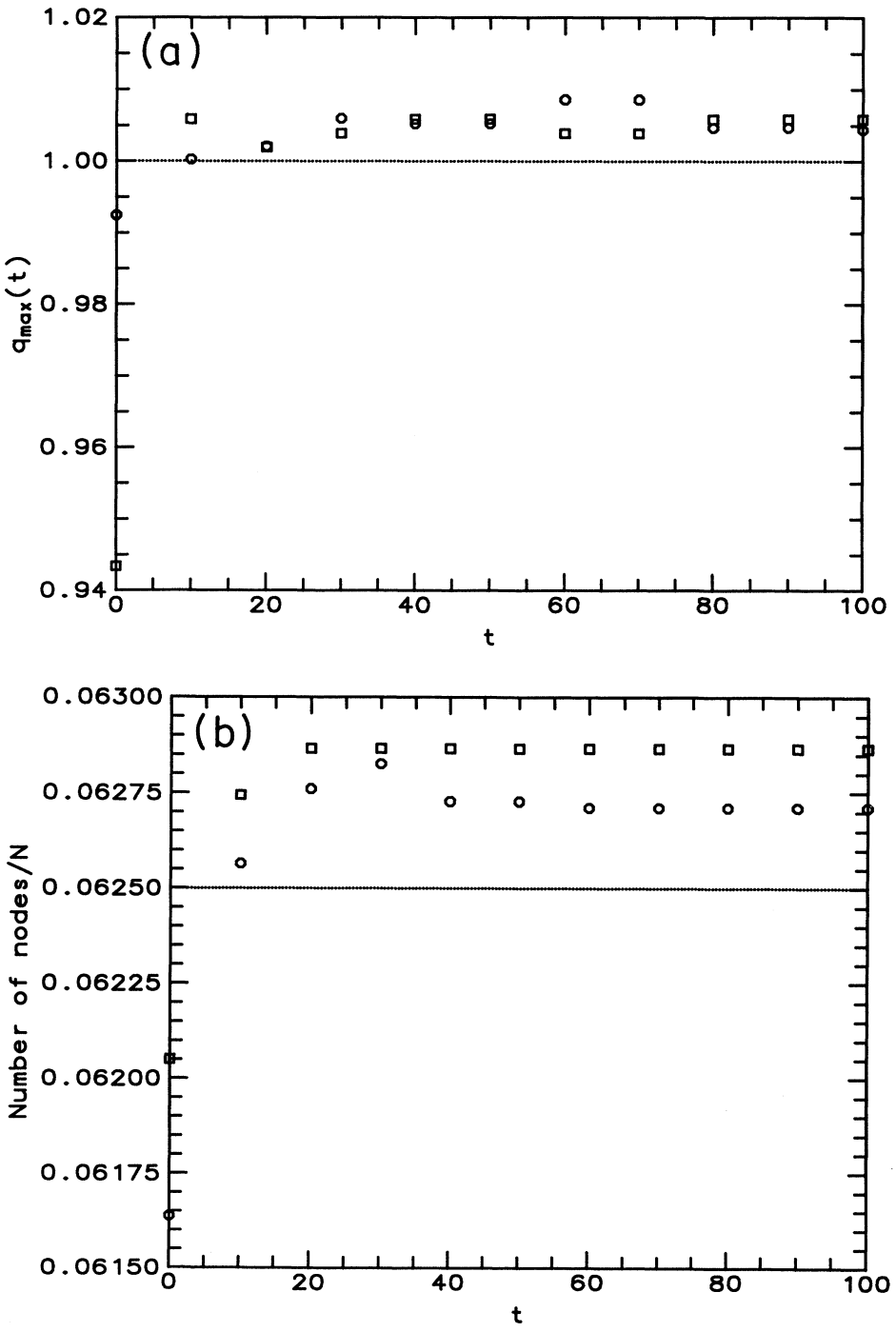


FIG. 2. (a) Location of the maximum of the power spectrum $q_{max}(t)$ for $\epsilon=0$. ○ corresponds to $N=8192$, and □ to $N=1024$. (b) Number of nodes of $y(x,t)$ as a function of time also for $\epsilon=0$. ○ corresponds to $N=8192$, and □ to $N=1024$. The dotted line shows the number of nodes of a periodic function of wave number $q = q_0$.

well-defined periodicity, separated by regions in which $|y(x,t)|$ is small. It is conceivable that these regions could act as effective boundary conditions and further restrict the range of allowed periodicities.

## III. NUMERICAL SOLUTION OF THE STOCHASTIC SWIFT-HOHENBERG EQUATION

A number of features of the transient and stationary solutions of the deterministic equation discussed in Sec. II do not hold for $\epsilon > 0$. For example, random fluctuations are expected to be important during the early stages after the instability for a range of time that depends on the relative amplitude of the fluctuations and on the solution itself. When monitoring the evolution of a single run starting from a given initial condition, one observes that any dependence of the final stationary solution on the initial condition is therefore removed, in contrast with the case $\epsilon=0$ [7]. The initial regime following the instability is well described by the linearization of Eq. (1). At intermediate times, however, the power spectrum $P(q,t)$ of a single run remains broad and its maximum changes as a function of time, reflecting the nonlinear competition among the various Fourier components of the configuration $\{y_i(t)\}$. At late times, configurations are expected to appear with a known stationary probability [given in Eq. (19)], as it will be discussed in more detail below. The asymptotic stationary power spectrum remains wide, indicating that the stationary configurations cannot be characterized by a single wave number.

The details of the numerical solution, boundary, and initial conditions are identical to those given in Sec. II. The random variable $\eta_i$ has been obtained by using the Box-Mueller transformation [16]. Most of our calculations have been performed with $\epsilon=0.1$, although we have also studied the cases $\epsilon=0.05$, 0.2, 0.3, and 0.4.

In order to better illustrate the character of the emerging solutions, we have calculated a local characteristic wave number. We first perform the following transformation:

$$\tilde{y}_i(x_0,t) = e^{-(x_i-x_0)^2/\beta^2} y_i(t) \ , \tag{14}$$

where $0 \le x_0 \le L$ and $x_i = (i-1)\Delta x$, $i = 1,\ldots,N$. The width $\beta$ is of the order of a few wavelengths. The Gaussian prefactor acts as a filter and selects only a portion of $y_i(t)$ around $x_0$ of width $\beta$ (other filter functions such as a square step have been used without altering the nature of the results). We next calculate the power spectrum of $\tilde{y}_i(x_0,t)$,

$$P_{x_0}(q,t) = \frac{1}{N}\left|\sum_{i=1}^{N} \tilde{y}_i(x_0,t) e^{-iqx_i}\right|^2 \ . \tag{15}$$

We show in Fig. 3 $P_{x_0}(q,t)$ for a typical configuration at long times ($t$=240) in a system with $N$=1024, $\epsilon$=0.2 and for $\beta$=10. This figure shows that the maximum of $P_{x_0}(q,t)$, which is related to the dominant periodicity around $x_0$, depends on $x_0$. Therefore, the configuration analyzed consists of different regions of a relatively well-defined periodicity. The boundaries between these regions are not sharp and their location is seen to be a function of time.

We have also analyzed the power spectrum, averaged over 20 initial conditions and realizations of the random variable $\eta_i$. The result shown in Fig. 4, indicates that there is still a preferred wave number at sufficiently long times but the distribution $P(q,t)$ is substantially broader than the case $\epsilon=0$. The power spectrum in the vicinity of $q_0$ can be fitted by

$$P(q,t) = A_1 e^{-\xi_1^2(q-q_0)^2} \ , \tag{16}$$

where $A_1$ and $\xi_1$ are adjustable parameters (solid line in Fig. 4). The tail region, on the other hand, can be fitted by

$$P(q,t) = \frac{A_2}{\xi_2^4(q^2-q_0^2)^2 + B_2} \ , \tag{17}$$

where $A_2, \xi_2$, and $B_2$ are also adjustable parameters.

Figure 5 shows the position of the maximum of $P(q,t)$ as a function of time for $\epsilon$=0.1 and $N$=8192. We find that $q_{\max} = 1.007 \pm 0.005$ at $t$=100, the latest time studied. The error is again estimated from the standard deviation of the values of $q_{\max}$ obtained for the 20 independent runs. This figure also shows that the average number of nodes as a function of time does not change significantly, and that at $t$=100, is $513 \pm 2$. The fact that the average number of nodes changes less in time than $q_{\max}$ suggests that the former quantity is a better characterization of the periodicity of the solution. In fact, the number of nodes for any individual run reaches a constant value for the finite duration of our run.

We have finally calculated the width of the power spectrum $W(t)$ for different values of $\epsilon$. We define $W(t)$ by

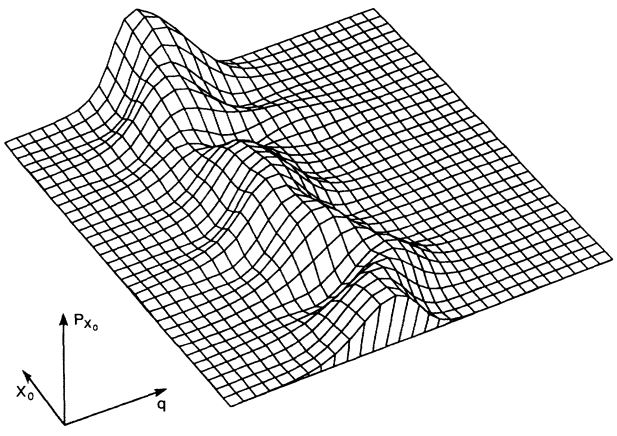


FIG. 3. Local spectrum $P_{x_0}(q,t)$ defined in Eq. (15). We have considered $N$=1024, $\epsilon$=0.2, $t$=240, and $\beta$=10. This figure shows that the power spectrum has a well-defined peak at a wave number that is a function of $x_0$. Therefore, the function $y_i(x)$ is locally periodic, but the local wave number varies as a function of $x$.

$$W(t)^2 = \frac{\int_0^\infty dq\ (q-q_0)^2\ P(q,t)}{\int_0^\infty dq\ P(q,t)} - \left(\frac{\int_0^\infty dq\ (q-q_0)\ P(q,t)}{\int_0^\infty dq\ P(q,t)}\right)^2 . \quad (18)$$

If $P(q,t)$ were well described by Eq. (16), $W^{-1}(t)$ would be proportional to $\xi_1$. This is not the case since the power spectrum is seen to decay much more slowly than exponentially for values of $q$ away from $q_0$ [Fig. 4 and Eq. (17)]. We show in Fig. 6(a) $W(t)$ as a function of time for several values of $\epsilon$ (the curves shown are averages over 20 independent runs for $\epsilon$=0.1 and 5 independent runs in the other cases). For the largest values of $\epsilon$, $W(t)$ reaches an asymptotic constant value for times that are accessible to our numerical calculations. For the smaller values of $\epsilon$ ($\epsilon$=0.05 and 0.1) $W(t)$ still decreases slightly at $t$=100. We show in Fig. 6(b) that $W^2(t=100)$ is approximately proportional to $\epsilon$ for the larger values of $\epsilon$. The fact that regions of different periodicity coexist (Fig. 3), and $1/W$ remains finite and smaller than $L$ (at least for the larger values of $\epsilon$) indicates that the stationary solutions of the stochastic equation do not have long-ranged periodicity. As a corollary, the question of wave-number selection is, in the presence of noise, ill defined when the aspect ratio is sufficiently large such that $1/W \ll L$.

In order to better clarify the nature of the asymptotic stationary solutions and to make sure that the Langevin dynamics embodied in Eq. (1) has given the truly asymptotic behavior for the finite range of time analyzed, we have implemented an alternative Monte Carlo calculation to obtain the stationary power spectrum. It follows from Eq. (7) that stationary configurations will appear with probability,

$$\mathcal{P}(\{y_i\}) = \frac{1}{Z}\exp\left(-\frac{\mathcal{L}(\{y_i\})}{\epsilon'}\right) , \quad (19)$$

where $Z$ is a normalization constant. In order to perform the Monte Carlo simulation we have again replaced the continuous function $y(x,t)$ by a discrete set of variables $\{y_i(t)\}$. The functional $\mathcal{L}(\{y_i\})$ is given by

$$\mathcal{L}(\{y_i\}) = \Delta x \sum_{i=1}^{N}\left[-\frac{\gamma^2-1}{2}y_i^2 + \frac{1}{4}y_i^4 - \left(\frac{y_{i+1}-y_i}{\Delta x}\right)^2 + \frac{1}{2}\left(\frac{y_{i+1}-2y_i+y_{i-1}}{\Delta x^2}\right)^2\right] . \quad (20)$$

The Monte Carlo sampling procedure that we have used in our calculations is known as heat bath Monte Carlo [17]. A succession of configurations are generated such that they appear with probability equal to $\mathcal{P}(\{y_i\})$. We select one site, say $k$, at random and change the value of $y_k$ while keeping the remaining $y_l, l \neq k$ fixed. Standard rejection techniques are used to obtain the new

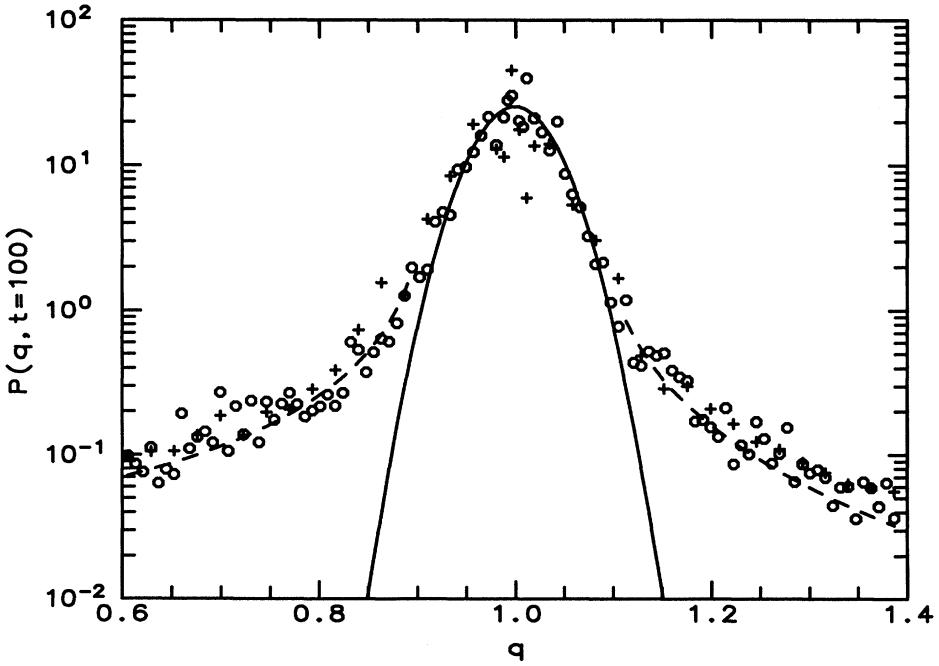


FIG. 4. Power spectrum $P(q,t)$ for $\epsilon$=0.1 and $N$=8192 at $t$=100, averaged over 20 independent runs. ○ denotes the solution to the Swift-Hohenberg equation, × corresponds to the power spectrum calculated by Monte Carlo methods, the solid line is the fit given in Eq. (16) with $\xi_1 \simeq 19$, and the dashed line the fit to Eq. (17) with $\xi_2 \simeq 6$.

value for the variable $y_k$. One Monte Carlo step (MCS) is defined to be N such attempts. We have studied the case $N$=8192 with periodic boundary conditions, and the same values of the parameters given above, namely $\gamma$=0.5, $\Delta x = 2\pi/32$, and, $\epsilon$=0.1. We have considered seven independent runs, each comprising 70 000 MCS's. We discard the configurations up to 35 000 MCS's and then average the power spectrum every 500 MCS's. The averaged $P(q,t)$ thus obtained has been further averaged over the seven independent runs. The power spectrum

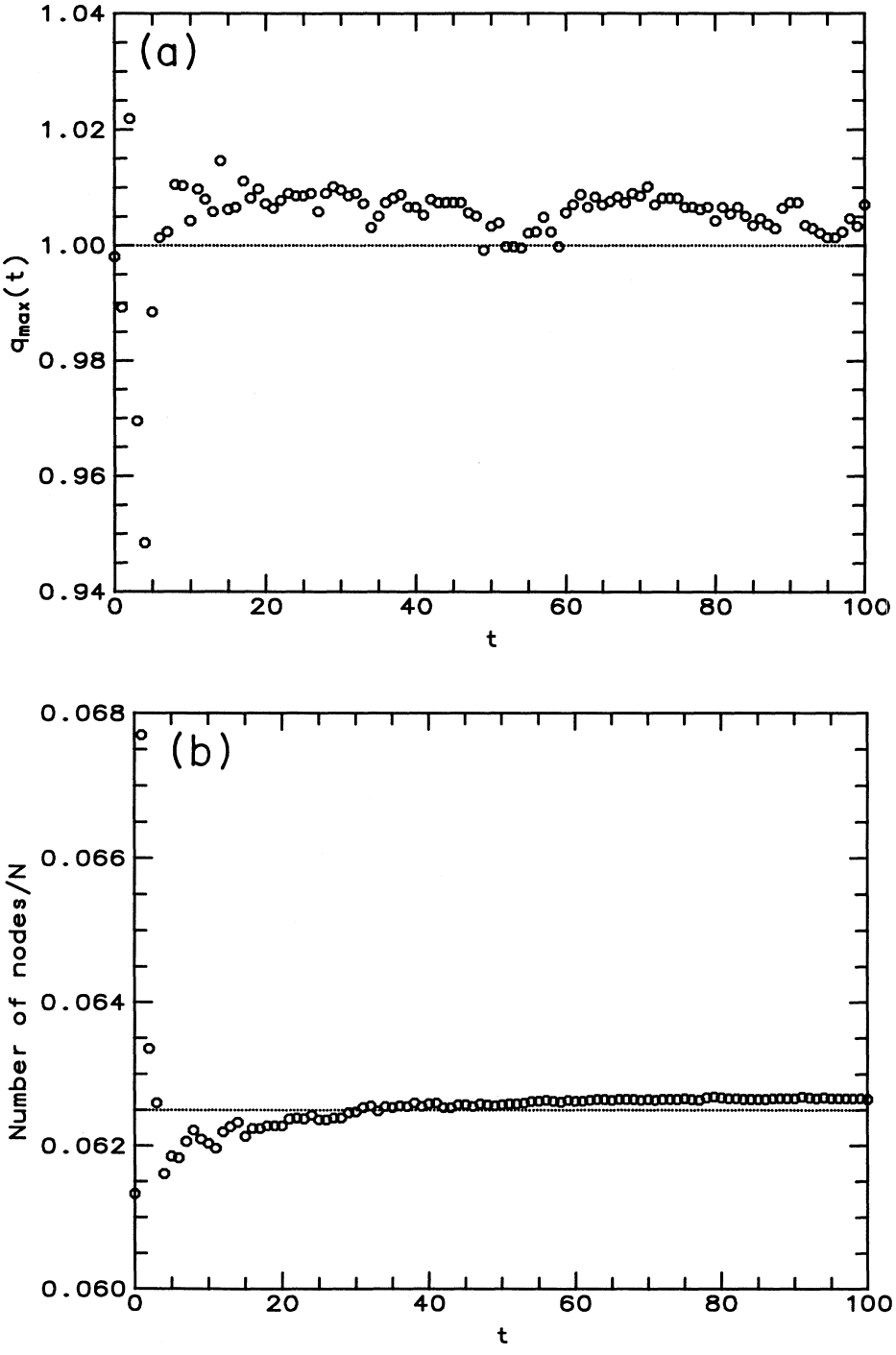


FIG. 5. (a) Location of the maximum of the power spectrum $P(q,t)$ for $\epsilon$=0.1 and $N$=8192. (b) Number of nodes of $y(x,t)$ as a function of time. The dotted line shows the the number of nodes of a periodic function of wave number $q = q_0$.

obtained is shown in Fig. 4, and it is in good agreement with the power spectrum obtained by direct integration of Eq. (1). Hence the distribution of solutions at long times given by direct integration of Eq. (1) yields a power spectrum that coincides, within the accuracy of our calculations, with that given by direct sampling of Eq. (19).

## IV. SUMMARY AND DISCUSSION

We conclude with several additional remarks. The nature of the solutions in the case of $\epsilon=0$ depends on the choice of boundary conditions. The boundary conditions that are realistic in the description of a convective insta-

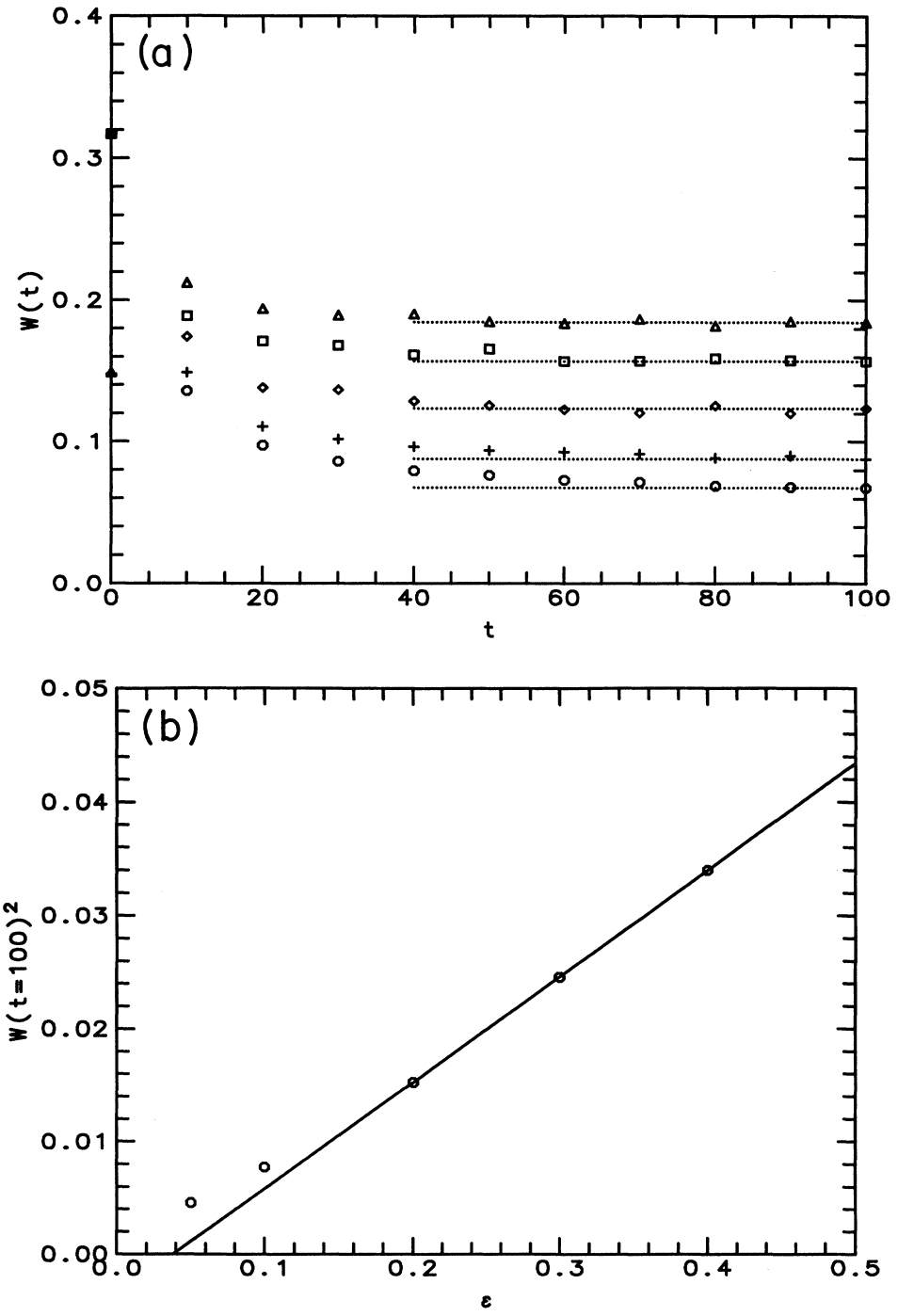


FIG. 6. (a) Width of the power spectrum $W(t)$ as a function of time for different values of $\epsilon$: ○, $\epsilon=0.05$; ×, $\epsilon=0.1$; ◇, $\epsilon=0.2$; □, $\epsilon=0.3$; and △, $\epsilon=0.4$. The dotted lines correspond to $W(t=100)$ for the various values of $\epsilon$. These values are shown again in (b) as a function of $\epsilon$.

bility in a finite experimental cell are given in Eq. (9), and are different than the boundary conditions used in the present study. Therefore, the distribution of wave numbers of the stationary solutions corresponding to a distribution of initial conditions need not be the same in both cases. We have studied an ensemble of initial conditions and found that for most of them, the wave number of the corresponding stationary solution is very close to $q_0$ (Fig. 2), but that other wave numbers are possible within a range $\sigma$=0.02. This range is much narrower than the band of configurations that are stable against the Eckhaus instability and is close to the range $q_+ - q_- \simeq 0.03$ (for $\gamma = 0.5$) given by Refs. [5] and [8] for *different* boundary conditions. A key mechanism in determining the selected wave number is the conservation law for the number of nodes at sufficiently late times. Our calculations support such a view and, in fact, we have observed that the number of nodes immediately after the initial linear regime completely determines the wave number of the asymptotic stationary solution.

In the case of $\epsilon > 0$, characteristic long-time configurations do not exhibit a well-defined periodicity. We have calculated a correlation length that measures the size of the regions over which these solutions can be characterized by a single periodicity and found it to be smaller than $L$. Consequently, we expect that our results and conclusions in this case are independent of the choice of boundary conditions. We find that the stationary power spectrum is well described by a Gaussian function in the vicinity of $q_0$ [Eq. (16)]. The tails, however, decay as a power law [Eq. (17)]. The width $W(t)$ increases with the amplitude of the fluctuations $\epsilon$. Even though $P(q,t)$ is broad and $W^{-1} < L$, we find that the average number of nodes does not change significantly in time (if $\epsilon$ is not too large) (Fig. 5). Conservation of the number of nodes in each individual run still holds at long times for sufficiently small $\epsilon$.

An important question that remains to be addressed is the possible different role played in the selection process by the wave number of the fastest growing mode in the linear regime $q_0$ and the wave number of the periodic configuration that minimizes the Lyapunov functional $q_{\min}$. For the value of $\gamma$ that we have used $q_0$ is almost identical to $q_{\min}$ and therefore their difference is well beyond the precision of our study. A possible alternative approach is to study the decay of an unstable periodic solution for which the wave number of the fastest growing mode in the linear regime is appreciably different than $q_{\min}$. Work in this direction is already in progress.

Finally we note that our results may strongly depend on the dimensionality. Fluctuations in convective states in fluid systems are effectively two dimensional since fluctuations in the direction parallel to the convective heat current are strongly suppressed. Therefore, a two-dimensional model is more appropriate than the model considered in this work. In particular, a two-dimensional equation allows the existence of topological defects, obviously not present in the one-dimensional case, that might affect both the selection mechanism of stationary solutions and their long-range order for finite values of $\epsilon$.

## ACKNOWLEDGMENTS

This international cooperation has been made possible by a grant from NATO, within the program "Chaos, Order and Patterns; Aspects of Nonlinearity," Project No. 890482. This work is also supported in part by the Supercomputer Computations Research Institute, which is partially funded by the U.S. Department of Energy under Contract No. DE-FC05-85ER25000, by the Dirección General de Investigación Científica y Técnica, under Contract No. PB 89-0424, and by the Universitat de les Illes Balears (UIB). Most of the calculations reported here have been performed on the 64k-node Connection Machine at the Supercomputer Computations Research Institute. We are indebted to Dr. Ken Elder and Dr. Martin Grant for many invaluable discussions, and to Dr. Pierre Hohenberg for useful suggestions. J.V. also acknowledges the hospitality of the UIB and of the Colonia Sant Jordi where part of this work was carried out.

* Present address: Department of Physics, McGill University, 3600 University Street, Montreal, Quebec, Canada H3A 2T8.

[1] S.A. Brazovskii, Zh. Eksp. Teor. Fiz. **68**, 175 (1975) [Sov. Phys.—JETP **41**, 85 (1975)]; J. Swift and P.C. Hohenberg, Phys. Rev. A **15**, 319 (1977).

[2] G. Ahlers, M.C. Cross, P.C. Hohenberg, and S. Safran, J. Fluid Mech. **110**, 297 (1981).

[3] M. Kerszberg, Phys. Rev. A **28**, 1198 (1983).

[4] M. de la Torre and I. Rehberg, Phys. Rev. A **42**, 2096 (1990); S. Rasenat, V. Steinberg, and I. Rehberg, *ibid.* **42**, 5998 (1990).

[5] Y. Pomeau and S. Zaleski, J. Phys. (Paris) **42**, 515 (1981).

[6] Y. Pomeau and P. Manneville, Phys. Lett. **75A**, 296 (1980).

[7] H.R. Schober, E. Allroth, K. Schroeder, and H. Müller-Krumbhaar, Phys. Rev. A **33**, 567 (1986).

[8] M.C. Cross, P.G. Daniels, P.C. Hohenberg, and E.D. Siggia, J. Fluid Mech. **127**, 155 (1983).

[9] Y. Pomeau and P. Manneville, J. Phys. (Paris) **40**, L609 (1979).

[10] For the ranges of $\gamma$ and $q$ studied in this paper, the stationary solutions found numerically for $\epsilon$=0 differ, for any $x$, by less than $10^{-3}$ with the first term of the series given in Eq. (3), the contribution of the remaining harmonics being negligible.

[11] W. Eckhaus, *Studies in Non-Linear Stability Theory*, Springer Tracts in Natural Philosophy Vol. 6 (Springer-Verlag, New York, 1965); L. Kramer and W. Zimmermann, Physica **16D**, 221 (1985); L. Kramer and P.C. Hohenberg, *ibid.* **13D**, 357 (1984).

[12] K. Tsiveriotis and R.A. Brown, Phys. Rev. Lett. **63**, 2048 (1989); note that this reference considers a complex modification of the Swift-Hohenberg equation.
[13] G. Dee and J.S. Langer, Phys. Rev. Lett. **50**, 383 (1983); E. Ben-Jacob, H.R. Brandt, G. Dee, L. Kramer, and J.S. Langer, Physica **14D**, 348 (1985).
[14] W. van Saarloos, Phys. Rev. A **37**, 211 (1988).
[15] K. Elder and M. Grant, J. Phys. A **23**, L803 (1990).
[16] G. Dahlquist and A. Björk, *Numerical Methods* (Prentice Hall, Englewood Cliffs, NJ, 1974), p. 453.
[17] M. Kalos and P. Whitlock, *Monte Carlo Methods, Volume I: Basics* (Wiley, New York, 1986).